

Development of the Johns Hopkins Xylophone Bar Magnetometer

Douglas A. Oursler, Dennis K. Wickenden, Laurence J. Zanetti, Thomas J. Kistenmacher, R. Ben Givens, Robert Oslander, John L. Champion, and David A. Lohr

A novel xylophone resonating bar magnetometer, invented by APL's Research and Technology Development Center, is being developed in collaboration with the Space Department into a compact, high-sensitivity, wide dynamic range sensor suitable for space physics applications. The magnetometer's principles of operation are presented and are demonstrated in experimental situations. The sensor uses the Lorentz force and the xylophone bar's mechanical resonance to yield subnanotesla sensitivity. This resonance technique offers large mechanical gains at the expense of bandwidth (typically a few hertz). However, the device can be used as a mixer to detect alternating magnetic fields. This capability is demonstrated at low frequencies (a few hertz) and at radio frequencies (a few megahertz). The sensor incorporates no magnetic materials and, therefore, can be used to detect small fields while rejecting large out-of-band signals. The resonator's temperature sensitivity is mitigated using feedback. The device is in an early engineering prototype stage. Eventually, using micro-machining and chip-on-board techniques, it is expected to be implemented as a "magnetometer on a chip." (Keywords: Lorentz force, Magnetic fields, Magnetometer, Resonator.)

INTRODUCTION

Although the field of magnetometry is mature, the need for miniature magnetic field sensors with subnanotesla sensitivity continues. The drive to smaller, higher-performance, and cheaper electronic devices has become a rallying cry in the space community and can be heard in other arenas as dissimilar as transportation, biomedicine, and munitions. The development of true chip-based high-sensitivity three-axis

magnetometers, magnetometer arrays, and gradiometers could profoundly change the way magnetic field sensing is implemented and allow a proliferation of these sensing devices for many applications.

Terrestrial applications of such a high spatial resolution array would, for example, allow imaging by physicians of neuron charge transfer in the brain or the guiding of unseen surgical instruments in the body. Such

an array might be used to image currents around sites of corrosion on the surface of insulation-clad pipe in a refinery. Small magnetometer arrays might also be used in vending machines to sense the erroneous magnetic signature of counterfeit money. Swarms of sea-based magnetometers carried by miniature autonomous probes might track surface and subsurface activity.

Spaced-based needs include the measurement of naturally occurring magnetic fields from strong planetary sources, such as the Earth's ($35 \mu\text{T}$), to relatively weak interplanetary fields ($\approx 1 \text{ nT}$). A spacecraft's magnetometer is perhaps its most important measurement device. Earth-orbiting satellites use magnetometers to calculate their orientation and altitude. Probes such as the Near Earth Asteroid Rendezvous (NEAR) use magnetometers to study the strength and variations of magnetic fields to discern the origins of stellar bodies.¹

Increasingly, there is a need to measure a spacecraft's artificially generated fields. These locally emanating fields stem from spacecraft system electrical currents and residual structural magnetization. For body-mounted magnetometers like those on NEAR, the spacecraft-induced fields add noise to the background and interfere with the intended primary measurement.¹ A system of strategically located body-mounted micro-magnetometers might offer several advantages. Primarily, such a sensor array could be used in an autocorrection effort to compensate for local effects. A secondary benefit is that the measurement of a spacecraft's fields would have significant diagnostic value, enabling engineers to monitor onboard activities such as deployment of appendages (i.e., solar panels or antennas).

Sensitive micro-magnetometers will enable new generations of small, compact, boomless spacecraft to be built. Eventually, a multitude of micro-spacecraft, each carrying a magnetometer, will map large-scale temporal and spatial changes (e.g., the curl) in the fields of space. Such spacecraft constellations are needed to forecast space weather.

Traditionally, spacecraft magnetic field measurements have been performed by fluxgate magnetometers^{2,3} and vapor magnetic field sensors.⁴ However, efforts to miniaturize sensor size and mass have been limited by construction difficulties and loss of sensitivity. Truly miniature sensors with subnanotesla sensitivity based on these techniques may not be possible.

The goal of miniaturizing magnetometers has led to the development of other new devices such as piezoresistive⁵ and magnetostrictive⁶ cantilevers, magnetoresistive films,⁷ and magnetometers based on electron tunneling effects.⁸ The sensitivity of these methods, however, has not reached the subnanotesla range. Conversely, superconductors can be used to create high-sensitivity magnetometers, but their cooling requirements typically limit their miniaturization.

Eventually, the full system is expected to be integrated onto one die and operate as a highly sensitive "magnetometer on a chip."

XYLOPHONE BAR MAGNETOMETER

Development

The resonating Xylophone Bar Magnetometer is one of many sensor concepts recently developed by APL's Research and Technology Development Center (RTDC). This novel and relatively simple device uses the Lorentz force to measure a particular magnetic field vector. It offers the potential of being lightweight and operating in a low power mode. True to its name, the device is based on a classical resonating xylophone bar, which can be scaled down to a small size (prototype sensor bars made from copper-beryllium [CuBe] foil are a few millimeters in size). The resulting small sensor elements can be employed in scanning or array configurations to measure magnetic field gradients or for magnetic imaging applications. This sensor concept is ideally suited to miniaturization using one of the many available microelectromechanical system (MEMS) technologies. (In a parallel effort, the RTDC is in the early stages of developing MEMS xylophone bars constructed of polysilicon and lead-zirconate-titanate.) Finally, the xylophone magnetometer operates without using any magnetic materials (ferrites), which prevents sensor saturation in the presence of large fields.

To date, the development of the Xylophone Bar Magnetometer has concentrated on the miniaturization of the sensing element and an understanding of the device's capabilities. The sensor uses conventional breadboard electronics to facilitate development. A reduction in mass and volume of the electronics can eventually be achieved with standard custom chip and bare-die advanced packaging technologies and poses no limiting factors. Details of the sensor's early development have been reported,⁹⁻¹¹ and patents are pending.

Principles of Operation

The Xylophone Bar Magnetometer operates by using the Lorentz force to transduce current flow through a wire crossing a magnetic field into a mechanical force, which results in displacement of the wire. This same interaction drives an electric motor. However, in small magnetic fields the current would have to be tremendous to yield a displacement that is detectable. The genius of the APL device is that it uses a classical xylophone bar resonator as the current-carrying element. Therefore, when an alternating current at a frequency matching the bar's mechanical resonance is applied to a bar that traverses a constant magnetic field,

the resultant alternating Lorentz force sets the xylophone into mechanical oscillation. This use of mechanical resonance acts as a gain mechanism and allows a small oscillating force to yield a detectable displacement.

The xylophone bar, shown in Fig. 1, is constructed to behave as a “free floating” beam with unclamped ends. The supports, which act as electrical contacts, are placed at the nodal locations for the fundamental mode of oscillation. These locations are 22.4% of the bar’s length from each end. The fundamental resonance frequency is¹²

$$f_0 = \frac{22.4}{2\pi} \sqrt{\frac{EI_a}{w\ell_b^4}} = \frac{1.029b}{\ell_b^2} \sqrt{\frac{E}{\rho}}, \quad (1)$$

where

E = Young’s modulus (N/m^2),

ℓ_b = beam length (m),

I_a = area moment of inertia ($= ab^3/12$),

w = uniform load per unit length ($w = \rho ab$) due to the mass of the bar, and

ρ , a , and b = the bar’s density, width, and thickness, respectively.

When a current I is driven through the xylophone bar in the presence of a magnetic field \vec{B} , as shown in Fig. 1, the resulting Lorentz force F is¹³

$$\vec{F} = \ell_c (\vec{I} \times \vec{B}); \quad \therefore F = \ell_c IB \sin(\Phi). \quad (2)$$

Here the angle between \vec{I} and \vec{B} is Φ . The force \vec{F} is perpendicular to the plane containing \vec{I} and \vec{B} . The term ℓ_c is the length of the portion of the xylophone

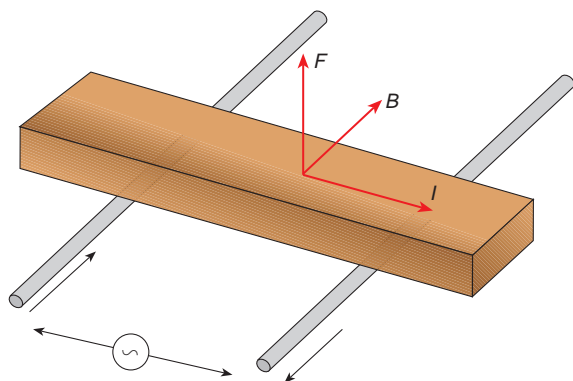


Figure 1. The Xylophone Bar Magnetometer’s current and magnetic flux interaction. I , B , and F represent electric current, magnetic flux, and the Lorentz force, respectively.

bar that contains current, i.e., the distance between the supports.

When a static force is applied to the xylophone bar, the midpoint deflection (i.e., constant current, dc, and constant magnetic field) is given by the beam equation¹²

$$d_{dc} = \frac{F \ell_c^3}{48I_a E}. \quad (3)$$

If the Lorentz force is alternating at a frequency f , then the amplitude of the midpoint bar deflection is given by

$$d_0 = \frac{d_{dc}}{\sqrt{[1 - (f/f_0)^2]^2 + (f/Qf_0)^2}}, \quad (4)$$

where f_0 is the mechanical resonance frequency given by Eq. 1, and Q is the resonance quality factor (Q factor). This equation indicates that when the force and resonance frequencies are equal, the beam deflection will approach $Q \cdot d_{dc}$. Q is determined by the bar’s material parameters, such as ductility, and construction factors, such as the placement and width of the supports.

If \vec{I} and/or \vec{B} are sinusoidally time-varying, their magnitudes can be rewritten as $I = I_0 \sin(2\pi f_i t)$ and $B = B_0 \sin(2\pi f_b t)$, where f_i and f_b are the current and magnetic field frequencies, respectively, and t is time. In this case, the second half of Eq. 2 can be rewritten as

$$F = \left[\frac{\ell_c B_0 I_0}{2} \sin(\Phi) \right] \times \left\{ \cos[(f_i - f_b)2\pi t] - \cos[(f_i + f_b)2\pi t] \right\}. \quad (5)$$

The first cosine term of Eq. 5 represents the force induced on the xylophone bar at the “beat” frequency. The second cosine term represents the “sum” frequency. These terms come from the multiplication of \vec{I} and \vec{B} in the cross product and represent frequency “mixing.” Therefore, when $(f_i + f_b)$, $(f_i - f_b)$, or $(f_b - f_i)$ equals f_0 , the xylophone will vibrate and, with the use of appropriate detection electronics, will generate a signal.

It is evident from these equations that, at resonance, the deflection of the xylophone bar is linearly proportional to the current through the bar, the magnetic field component perpendicular to the bar, and the Q factor. It is also apparent that the device may be used as a mixer to detect time-varying magnetic fields if the bar

current frequency is chosen correctly (Eq. 5). Both of these behaviors have been experimentally demonstrated in prototype devices. A single device has measured static (dc) magnetic fields from below 1 nT to above 1 T by simply adjusting the bar current amplitude. In another experiment, the xylophone magnetometer has been implemented as a mixer to detect sinusoidally varying magnetic frequencies of up to 10 MHz.¹⁴ The upper frequency limit seems only to depend on the bar's skin depth.

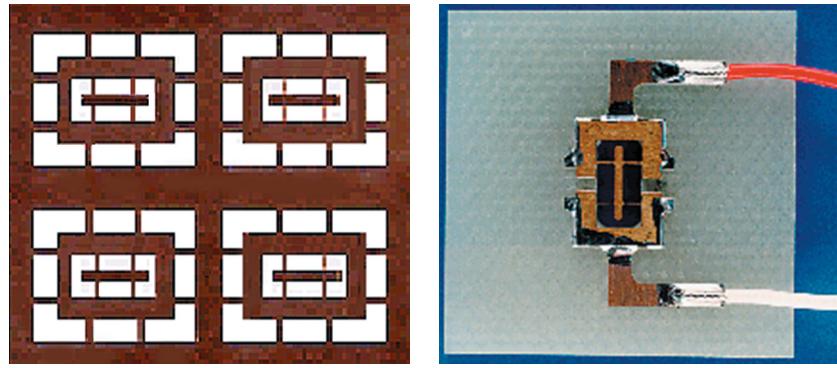


Figure 2. Freshly chemically milled CuBe xylophone bars (left) and a finished, board-mounted bar ($5 \times 0.5 \times 0.25$ mm thick).

Sensor Element

The concept for the resonating Xylophone Bar Magnetometer is fully capable of being miniaturized by a variety of technologies, including conventional fabrication using electrostatic discharge machining and chemical milling. Today, engineering prototype xylophone bars are simply and effectively fabricated from nonmagnetic CuBe foils by chemical milling. To increase reflectivity and retard oxidation, a multilayer film (Ti/Pt/Au) is deposited on the surface. Typically, these xylophone bars are $5 \times 0.5 \times 0.25$ mm, with Q values of approximately >7000 and resonant frequencies around 44 kHz. Figure 2 shows a portion of the CuBe foil after milling and a finished xylophone bar mounted on a modified PC board as it is used in the sensor.

Deflection of the xylophone bar is generally determined by optical methods. The light from a laser diode is reflected off one of the bar's ends and onto a position-sensitive (photo) detector (PSD). A lock-in amplifier is used to extract the final signal. Figure 3 illustrates the response of a xylophone bar magnetometer and a

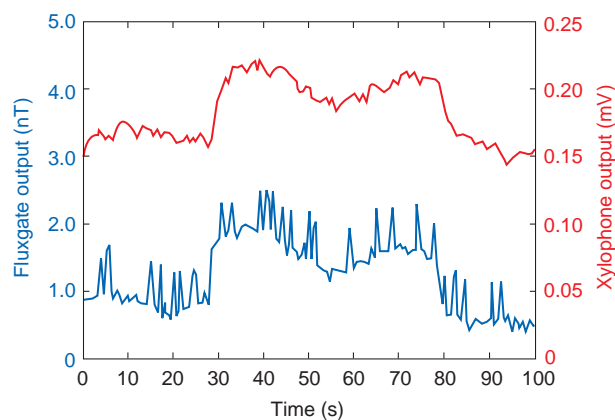


Figure 3. The response of a xylophone bar (top curve) and fluxgate magnetometer (bottom curve) to a 1-nT change in magnetic field.

fluxgate magnetometer to magnetic field variation on the order of 1 nT. Here, the xylophone bar current amplitude is 1 A and the xylophone system bandwidth is a few hertz. The fluxgate has a wider bandwidth, approximately 100 Hz. (The spikes on the fluxgate signal are caused by the undersampling of the 60-Hz background field by the digitizer.) The displacement frequency response (magnitude and phase angle) for a typical 5-mm-long chemically milled xylophone bar is shown in Fig. 4.

The Xylophone Bar Magnetometer has also been demonstrated as a frequency mixer. Figure 5 shows the sensor's response to low-frequency sinusoidal magnetic fields of 2, 10, and 20 Hz relative to the resonance frequency f_0 . The detection system lock-in amplifier is *always* tuned to the xylophone frequency f_0 . This figure was generated by sweeping the xylophone drive current frequency. The central line at the xylophone resonant frequency is due to the incomplete nulling of

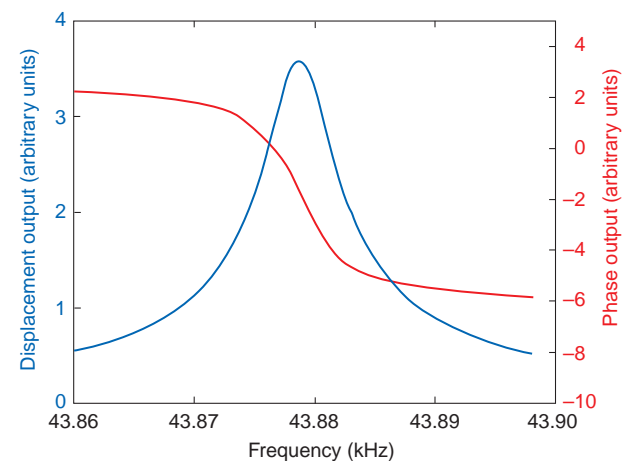


Figure 4. A xylophone bar displacement spectrum (magnitude and phase angle) in a static magnetic field versus the drive current frequency.

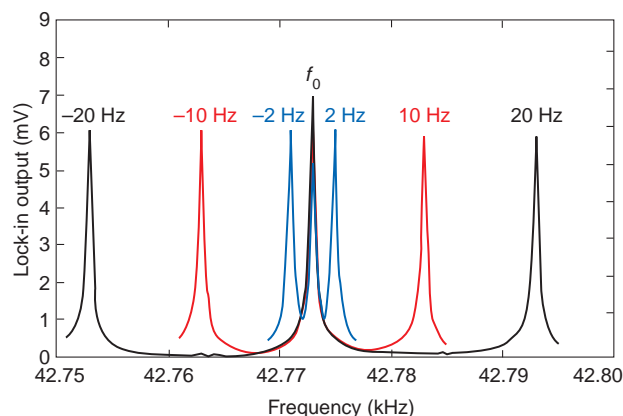


Figure 5. The amplitude of the xylophone magnetometer response to low-frequency sinusoidal magnetic fields (2, 10, and 20 Hz) as a function of drive current frequency. The Earth's (constant) field is seen at f_0 .

the Earth's magnetic field. (Nulling is accomplished by orienting the magnetometer's axis of sensitivity in an east–west direction.) Each of the three magnetic field components has a “sum” and “beat” frequency response (Eq. 5).

Figure 6 depicts the response of the xylophone magnetometer to a high-frequency sinusoidal (1-MHz) magnetic field as a function of drive current frequency. In this case, the magnetic field frequency f_b is much greater than the xylophone resonance frequency f_0 . Therefore, two “beat” conditions exist where the magnitude to the difference frequency, $(f_i - f_b)$ or $(f_b - f_i)$, equals f_0 . The insert in Fig. 6 shows the two resonances overlaid side-by-side for comparison purposes. Although the Q s of the resonances are as expected, the difference in amplitude of the sidebands is unforeseen.

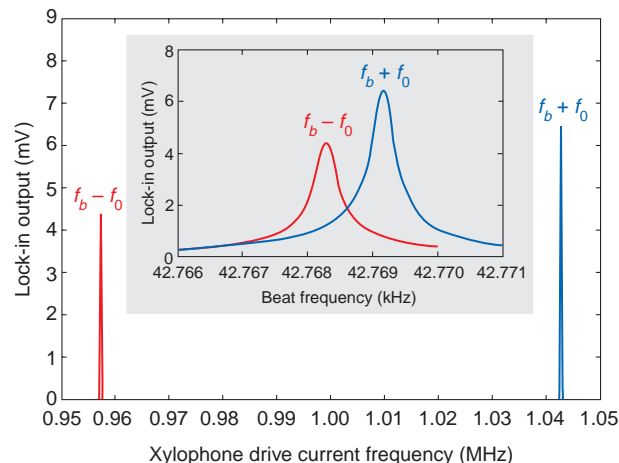


Figure 6. The amplitude of the xylophone response to a high-frequency sinusoidal (1-MHz) magnetic field as a function of drive current. The insert shows the two resonances overlaid side-by-side for comparison purposes.

This behavior is (tentatively) being attributed to skin depth variations at these frequencies and is presently being investigated. However, we believe that the skin depth phenomenon represents an upper operating frequency limit of the xylophone magnetometer.

Engineering Prototype

The development of the Xylophone Bar Magnetometer toward a space-qualified instrument has been a major goal of recent joint Space Department and RTDC research and development efforts. In the last year a demonstration model single-axis xylophone magnetometer using 5-mm CuBe bar resonators and conventional electronics has been constructed. Figure 7 shows the sensor head and electronics enclosure (including power-supply conditioning) of the device. As a compromise between size and cost, the electronics are constructed of conventional components. The system represents a significant step away from larger ones used during basic development that incorporated multiple rack-mounted pieces of equipment.

A schematic of the engineering prototype Xylophone Bar Magnetometer is shown in Fig. 8. The system's sensor body contains a xylophone bar, an optical deflection sensor, a calibration coil, and pressure and temperature sensors. The main electronics enclosure contains the microprocessor and other electronics for sensor self-tuning and signal processing.

The sensor begins operation with the microprocessor tuning the amplitude and frequency output of the digital sine wave synthesizer. This signal drives a step-down transformer to provide an alternating current to the xylophone bar. When a magnetic field is present and the frequency tuning is correct, the bar begins to vibrate. This motion is detected using optical beam deflection. The light from a laser diode is focused by a lens and reflected from the bar to form a spot on the PSD. The currents from the PSD's two outputs

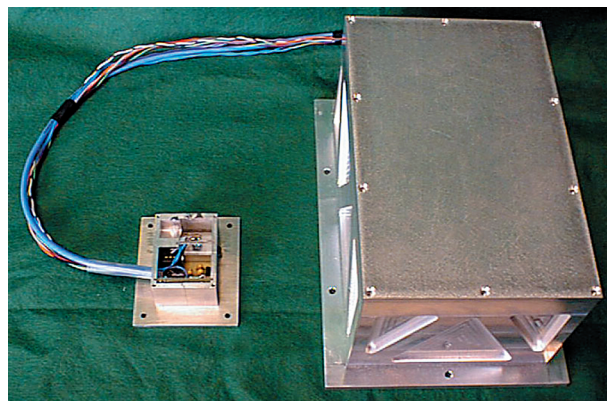


Figure 7. The single-axis prototype magnetometer sensor head (left; $\approx 5 \times 3.5$ cm) and electronics enclosure (right).

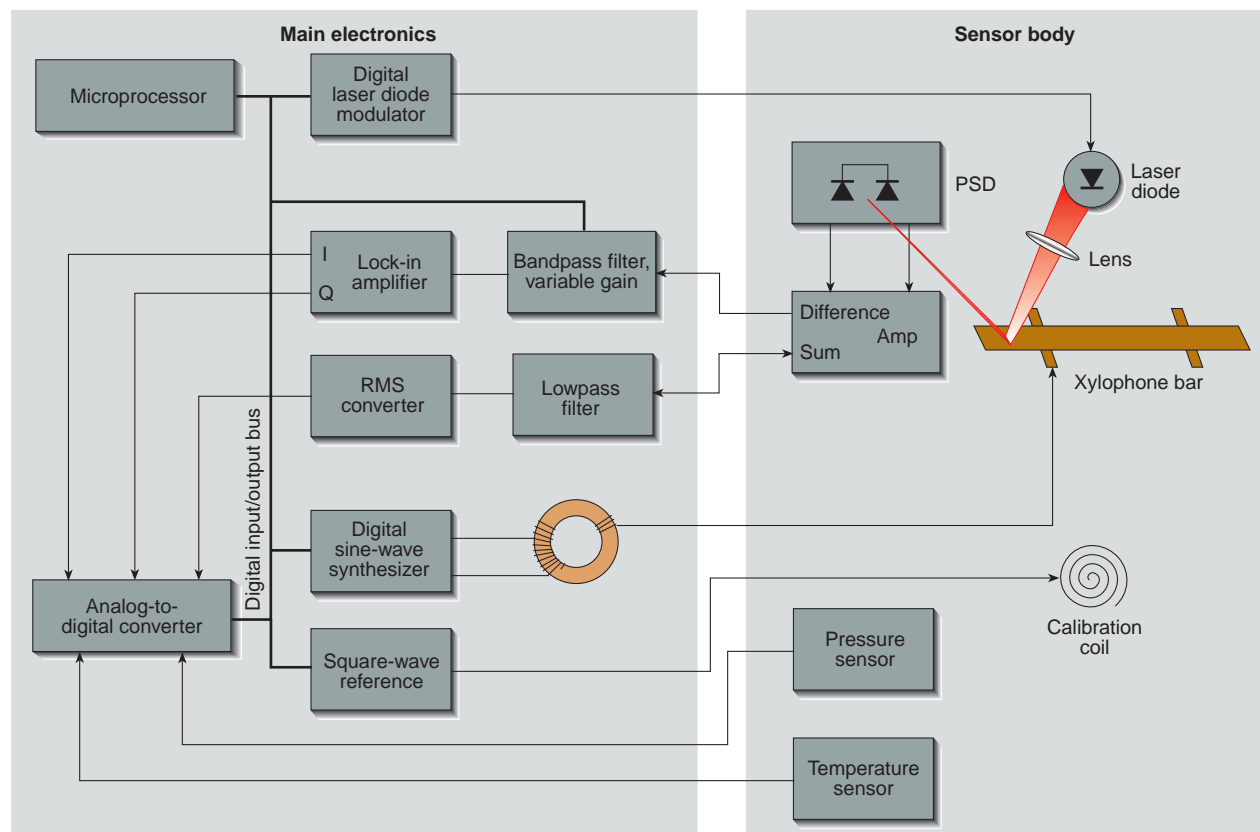


Figure 8. The sensor head and main electronics for the engineering prototype Xylophone Bar Magnetometer (PSD = position-sensitive [photo] detector; I and Q = in phase and quadrature phase, respectively).

vary proportionally to the beam spot's lateral position on the detector. Using a difference amplifier, a signal is generated which indicates the beam spot's motion and, therefore, the bar's motion. This signal is filtered, demodulated by a lock-in amplifier, digitized, and processed to provide magnetic field magnitude and phase angle data.

At start-up, the sine wave synthesizer sweeps through a range of frequencies known to include the bar's mechanical resonance frequency. This action produces a table of data similar to the data depicted in Fig. 4. The phase angle that corresponds to the peak of the resonance is stored and used as a reference point for tuning in the feedback loop. Under normal operating conditions, the sine wave synthesizer is tuned so that the Lorentz force frequency matches the bar's mechanical resonance frequency. The magnetometer's sensitivity is magnified by simply increasing the drive current of the xylophone bar.

The system is embellished in several ways to improve performance. The laser diode is modulated at a microprocessor-controlled frequency. This technique is used to minimize cross-talk between the xylophone drive current and the lock-in detection system. The PSD sum signal, which is an indicator of the total light on the detector, effectively monitors the laser diode's health

and the quality of the bar's reflective coating. Pressure and temperature sensors are used to log sensor conditions during testing. Finally, the calibration coil is used to provide a small alternating reference field of known amplitude and frequency. This tuning standard is used during the start-up/initialization cycle.

FUTURE GOALS

In the next year, a three-axis sensor will be constructed with techniques similar to those used to build the present prototype. CuBe xylophone bars, along with conventional surface-mount electronics, will be used to demonstrate that three bars of different frequencies can operate in close proximity. This system will represent a final stage in the magnetometer's "proof of concept" development.

Subsequent efforts are expected to concentrate on integration and miniaturization. The MEMS xylophone bars (from parallel RTDC research efforts) will be incorporated into the sensor system. Early integration of the sensor and microelectronics is already in progress. High-sensitivity capacitive and piezoelectric pick-up schemes are under active development as well. Figure 9 shows an electron micrograph of a MEMS xylophone bar. Eventually the full system is expected

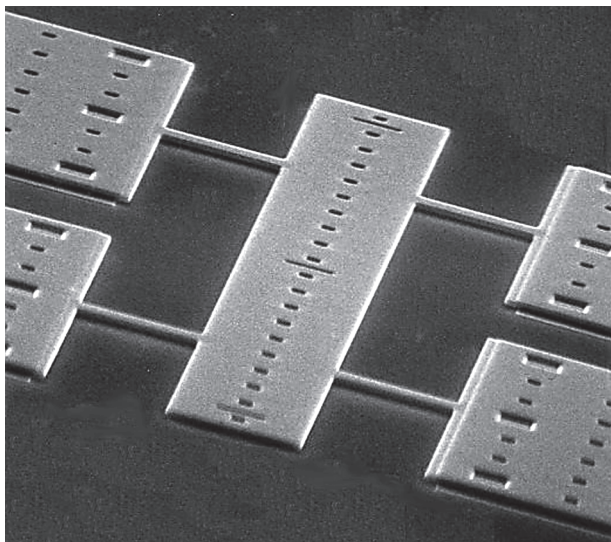


Figure 9. An electron micrograph of a MEMS xylophone bar made of polysilicon.

to be integrated onto one die and operate as a highly sensitive “magnetometer on a chip.”

APL’s Xylophone Bar Magnetometer is a new, highly sensitive method of detecting magnetic fields. The system uses the Lorentz force and the mechanical resonance of a miniature xylophone bar to make sub-nanotesla magnetic field measurements. The magnetometer’s sensitivity as well as its “mixing” capability have been demonstrated. A “stand-alone” sensor system has been constructed using conventional electronics and small CuBe xylophone bars to test operating and self-tuning concepts. Soon, the marriage of this system with the RTDC’s MEMS effort is expected to produce a highly compact sensor. This integration will provide three-axis systems and one- or two-dimensional sensor arrays for magnetic imaging. The ultimate goal

of single sensor systems is to provide an entire magnetometer on a chip.

REFERENCES

- ¹Lohr, D. A., Zanetti, L. J., Anderson, B. J., Potemra, T. A., and Acuna, M. H., “The NEAR Magnetic Field Instrument,” *Johns Hopkins APL Tech. Dig.* **19**(2), 136–141 (1998).
- ²Acuna, M. H., “Fluxgate Magnetometers for Outer Planet Exploration,” *IEEE Trans. Magnetics* **MAG-10**, 519–523 (1974).
- ³Acuna, M. H., Connerney, J. E., Wasilewski, P., Lin, R. P., Anderson, K. A., et al., “Mars Observer Magnetic Field Investigation,” *J. Geophys. Res.* **97**, 7799–7814 (1992).
- ⁴Smith, E. J., Marquedant, R. J., Langel, R., and Acuna, M., “Aristoteles Magnetometer System,” *Proc. Workshop on Solid Earth Mission ARISTOTELES*, ESA SP-329 (1991).
- ⁵Rossel, C., Bauer, P., Zech, D., Hofer, J., Willemin, M., and Keller, H., “Active Microlevers as Miniature Torque Magnetometers,” *J. Appl. Phys.* **79**, 8166–8173 (1996).
- ⁶Osiander, R., Ecelberger, S. A., Givens, R. B., Wickenden, D. K., Murphy, J. C., and Kistenmacher, T. J., “A Microelectromechanical-Based Magnetostrictive Magnetometer,” *Appl. Phys. Lett.* **69**, 2930–2931 (1996).
- ⁷Yang, F. Y., Liu, K., Hong, K., Reich, D. H., Seanson, P. C., and Chien, C. L., “Large Magnetoresistance and Field Sensing Characteristics of Electrodeposited Single-Crystal Bismuth Thin Films,” *Science* (in press).
- ⁸Miller, L. M., Podosek, J. A., Kruglick, E., Kenny, T. W., Kovacic, J. A., and Kaiser, W. J., “A μ -Magnetometer Based on Electron Tunneling,” in *Proc. IEEE Workshop on Micro Electro Mechanical Systems*, pp. 467–472 (1996).
- ⁹Givens, R. B., Murphy, J. C., Osiander, R., Kistenmacher, T. J., and Wickenden, D. K., “A High Sensitivity, Wide Dynamic Range Magnetometer Designed on a Xylophone Resonator,” *Appl. Phys. Lett.* **69**, 2755–2757 (1996).
- ¹⁰Wickenden, D. K., Givens, R. B., Osiander, R., Champion, J. L., Oursler, D. A., and Kistenmacher, T. J., “MEMS-Based Resonating Xylophone Bar Magnetometers,” in *SPIE Conf. Proc. Micromachined Devices and Components IV*, Vol. 3514, pp. 350–358 (1998).
- ¹¹Wickenden, D. K., Kistenmacher, T. J., Osiander, R., Ecelberger, S. A., Givens, R. B., and Murphy, J. C., “Development of Miniature Magnetometers,” *Johns Hopkins APL Tech. Dig.* **18**(2), 271–277 (1997).
- ¹²Young, W. C., *Roark’s Formulas for Stress and Strain*, 6th Ed., McGraw-Hill, New York (1989).
- ¹³Reitz, J. R., Milford, F. J., and Christy, R. W., *Foundations of Electromagnetic Theory*, 4th Ed., Addison-Wesley, New York (1992).
- ¹⁴Givens, R. B., Wickenden, D. K., Oursler, D. A., Osiander, R., Champion, J. L., and Kistenmacher, T. J., “Heterodyne Detection of Alternating Magnetic Fields with a Resonating Xylophone Bar Magnetometer,” *Appl. Phys. Lett.* **74**, 1472–1477 (1999).

ACKNOWLEDGMENTS: The authors would like to thank Dr. Joe Suter and the Sensors Thrust Area, Internal Research and Development Committee, for their considerable support of the magnetometer’s development. We would also like to thank Jeff Will (SER), Rick Edwards (TSE), David Lee (TSE), and Doug Dawson (TSM) for their substantial assistance in building these devices on site.

THE AUTHORS



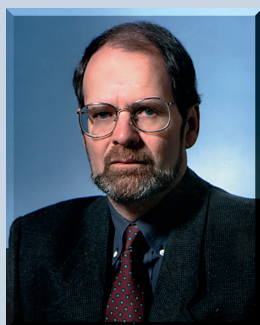
DOUGLAS A. OURSLER received a B.S. in electrical engineering and computer science from The Johns Hopkins University in 1987 and an M.S. in electrical engineering from the University of Virginia. He returned to Hopkins to receive an M.S. and later a Ph.D. in materials science in 1996. As a post-doctoral fellow, he continued his research in microwave and electromagnetic techniques of nondestructive testing. Dr. Oursler co-founded a small business that developed a novel laser contouring system to map automotive body panels for the automotive and steel industries. In 1997, he joined APL’s Senior Staff in the Space Department. Since then he has been involved with the testing of the all-polymer and hybrid batteries, the development of the Xylophone Bar Magnetometer for space applications, and the investigation of optical methods for missile launch point detection. His e-mail address is douglas.oursler@jhuapl.edu.



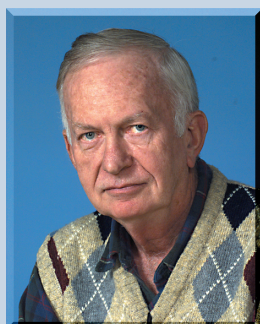
DENNIS K. WICKENDEN is a physicist in the Sensor Science Group of the APL Research and Technology Development Center. He received his B.Sc. and Ph.D. degrees from the Imperial College of Science and Technology (University of London) in 1962 and 1965, respectively. After a post-doctoral fellowship at the University of Notre Dame, he worked at the GEC Hirst Research Centre in England on the growth, characterization, and application of a variety of compound semiconductors. In 1985, he served as senior scientist at Crystal Specialties, Portland, OR, where he developed epitaxial growth equipment for the semiconductor industry. Dr. Wickenden joined APL as a Senior Staff physicist in 1987. His current research interests include growth and characterization of gallium nitride and related alloys and the development of microelectromechanical sensors. He was elected a Fellow of the Institute of Physics in 1973. His e-mail address is dennis.wickenden@jhuapl.edu.



LAWRENCE J. ZANETTI received a B.A. in physics from the University of Colorado in 1974 and an M.S. and Ph.D. in physics from the University of New Hampshire 1976 and 1978, respectively. He joined APL in 1978 and is a Principal Staff physicist and supervisor of the Magnetic Fields Section of the Space Physics Group. Dr. Zanetti was the principal investigator for the Freja Magnetic Field Experiment and instrument scientist for the NEAR Magnetometer Experiment. He is presently on special assignment at NASA Headquarters as program scientist for magnetospheric missions. His e-mail address is lanetti@hq.nasa.gov.



THOMAS J. KISTENMACHER is a Principal Professional Staff chemist in the APL Research and Technology Development Center. He obtained a B.S. in chemistry from Iowa State University and M.S. and Ph.D. degrees, also in chemistry, from the University of Illinois. During 1969–1971, he was a junior fellow in the A. A. Noyes Laboratory for Chemical Physics at the California Institute of Technology. From 1971 to 1982, he served on the faculties of both JHU and Cal Tech. Dr. Kistenmacher joined APL in 1982 and is currently with the Sensor Science Group. His principal research interests include the fabrication and analysis of thin films for a variety of structural, electronic, magnetic, and optical applications; X-ray diffraction; and the crystalline structure and structure–property relationships in several electronic and magnetic materials. His e-mail address is thomas.kistenmacher@jhuapl.edu.



R. BEN GIVENS is an Associate Staff member of the Sensor Science Group in APL's Research and Technology Development Center. He studied electronics while in the Army and later obtained an associate's degree in electronics from the Capitol Radio Engineering Institute. He joined APL in 1985 after working for the Maryland Electronic Manufacturing Company, where he focused primarily on evaluating instrument landing systems. Mr. Givens is the inventor of the Lorentz force magnetometer described in this article. His e-mail address is GIVENRB1@jhuapl.edu.



ROBERT OSIANDER is a physicist in the Sensor Science Group of the APL Research and Technology Development Center. He earned an M.S. in 1986 and a Ph.D. in 1991, both in physics, from the Technische Universitat Munchen in Munich, Germany, where he worked on thermal wave spectroscopy. He joined the Materials Science Group at APL as a post-doctoral fellow in 1991 and became a member of the Senior Professional Staff in 1995. Dr. Osiander's current research interests include the development of microwave and thermographic techniques for nondestructive evaluation and materials characterization, high-resolution microwave imaging, development and testing of microelectromechanical sensors, development of counterfeit deterrence features, electromagnetic interaction with biological systems, and the medical applications of thermographic methods. His e-mail address is robert.osiander@jhuapl.edu.



JOHN L. CHAMPION received a B.A. degree in physics from the University of Virginia in 1989 and an M.S. and Ph.D. from The Johns Hopkins University in materials science and engineering in 1995 and 1998, respectively. Before attending graduate school, he was employed by Science Applications International Corp., where he investigated the effects of radiation on electronic systems. Dr. Champion joined APL last spring as a JHU post-doctoral fellow in the Sensor Science Group of the Research and Technology Development Center. His current interests included design, fabrication, and characterization of MEMS devices for space systems. His e-mail address is john.champion@jhuapl.edu.



DAVID A. LOHR is a member of APL's Principal Professional Staff. He received a B.S. in physics from the University of Maryland in 1974. Before coming to APL in 1988, he worked at Northrop DSS and Litton Amecom. He was the lead engineer for the Freja Magnetic Field Experiment and the NEAR Magnetometer Experiment. Mr. Lohr is currently the lead engineer for the ACE EPAM Particle Experiment. He also participated in the JADE and Flare Genesis programs. His e-mail address is david.lohr@jhuapl.edu.